ISSN 1822-427X/eISSN 1822-4288
2023 Volume 18 Issue 1: 167–184
https://doi.org/10.7250/bjrbe.2023-18.593

THE BALTIC JOURNAL OF ROAD AND BRIDGE ENGINEERING
2023/18(1)

MODIFIED DEFLECTION THEORY FOR PRELIMINARY DESIGN OF SELF-ANCHORED SUSPENSION BRIDGES

MINMAO LIAO*, HUAILI PENG

School of Civil Engineering, Chongqing University, Chongqing, China

Received 11 December 2021; accepted 8 December 2022

Abstract. A modified deflection theory is developed for preliminary design of self-anchored suspension bridges. The proposed theory modifies the questionable approach of the existing theory considering the initial fabrication camber and overcomes the limitation that the hangers are assumed inextensible, which results in a stiffer bridge system and thus underestimation of the main cable and girder deflections. In addition, in order to avoid the inconvenience of solving a system of nonlinear equations iteratively for the preliminary design, the tower flexural stiffness is neglected rationally to obtain a system of linear equations only. With the aid of all force equilibrium and deformation compatibility conditions for the entire bridge system, the modified deflection theory is formulated. Its solution procedure is presented, which leads to a complicated sixth-order variable-coefficient ordinary differential equation, and a practical approximate solution to the equation is sought. To verify the proposed theory, a bridge example is investigated, and the results are compared to those from the previous deflection theory and complex finite element analysis. The comparisons demonstrate the effectiveness of the modified deflection theory.

Keywords: deflection theory, deformation compatibility, force equilibrium, preliminary design, self-anchored suspension bridge.

* Corresponding author. E-mail: liaom@cqu.edu.cn

Minmao LIAO (ORCID ID 0000-0002-8982-5994)

Introduction

Self-anchored suspension bridges (Ochsendorf and Billington, 1999) are particularly suitable for places where there are insufficient conditions for earth anchorages. Their main cables are secured directly to each end of the main girder. As a result, the main girder carries a compressive force transferred from the horizontal component of the cable tension, and live loads cause not only bending but also additional compression in the main girder. Taking this compression effect into account appropriately to avoid buckling instability of the main girder is of significance. Also, determinations of the additional compressive force, maximum vertical displacement and maximum bending moment in the main girder are of importance for preliminary design of the bridges.

Several theories (Buonopane and Billington, 1993), such as the Rankine's theory (only the main girder included) and elastic theory (the cable stiffness further considered), have been developed for the preliminary design of the conventional earth-anchored suspension bridge. Among them, the deflection theory (the vertical deflection of the cable further involved) is believed as the most sophisticated one so far. However, compared to numerous studies on the conventional earth-anchored suspension bridge based on the deflection theory (Jennings, 1987; Ulstrup, 1993; Clemente et al., 2000; Cobo del Arco and Aparicio, 2001; Wollmann, 2001; Choi et al., 2013; Shin et al., 2015; Gwon and Choi, 2018; Li and Liu, 2021; Zhang et al., 2021; Zhang et al., 2022), very little analytical attention has been paid to the self-anchored suspension bridge. Until 2015, Jung et al. (2015) just derived a deflection theory for the self-anchored suspension bridge considering the initial fabrication camber and tower flexural stiffness. Based on this theory, they further investigated the elastic stability behaviour of the bridge (Jung et al., 2017). On the other hand, a few numerical analyses (Kim et al., 2002; Kim et al., 2006; Romeijn et al., 2008; Han et al., 2009; Kim and Kim, 2012; Sun et al., 2015; Kim et al., 2019; Zhuang et al., 2021; Chen et al., 2022), mainly based on the finite element method (FEM), have been conducted for the self-anchored suspension bridge, but they are too demanding for the preliminary design.

In the deflection theory by Jung et al. (2015), the consideration of the initial camber is questionable. They introduced a girder deflection function, in addition to the initial camber, into the equilibrium equation of the main girder under dead loads (Equation (2) in the reference) but the initial camber was not included in the term of the second-order differentiation, rendering the initial cable geometry related to the initial camber (Equations (4b) and (5) in the reference) and the final deflection equation (Equation (9b) in the reference) not relevant to the whole initial camber function but only relevant to the camber values at the centre and ends of the span, through the horizontal tension of the main cable (Equation (6b) in the reference). This contradicts the conclusion that both the initial cable geometry and the horizontal tension of the main cable under the dead loads are irrelevant to the initial camber, derived from the equilibrium equation of the main cable under the dead loads (Equation (1) in the reference) with the assumption that the dead loads are uniformly distributed and carried by the main cable. One obvious evidence is that plugging the cable geometry (Equation (4b) in the reference) back into the equilibrium equation of the main cable (Equation (1) in the reference) arrives at not only the total dead loads but also an additional term related to the initial camber, which violates the assumption.

In addition, an unrealistic assumption has been made in the previous deflection theory, i.e. the hangers are inextensible. In this case, the deflection of the main girder is always the same as that of the main cable. This does not obey the truth that the hangers can be further elongated due to the hanger tension increment caused by live loads. Actually, this model simplification uses a rigid hanger hypothesis and results in a stiffer bridge system. Underestimation of the bridge deflection is anticipated.

Furthermore, the previous deflection theory considered the tower flexural stiffness explicitly by employing an equivalent horizontal spring at the tower top. This reflected the horizontal cable tension difference between two adjacent spans and might improve the accuracy of the design results. However, it was not mentioned how the value of the spring stiffness was determined, the consideration led to a system of nonlinear equations and the Newton-Raphson iteration method was required for solving the equations, which was inconvenient for the preliminary design. According to the cantilever beam-column theory (Timoshenko, 1947), when the compressive load applied to the top of the tower increases, the tower flexural stiffness reduces. Therefore, the enforcement of live loads, which increases the compression in the tower, will lower the tower flexural stiffness and in turn lower the cable tension difference. This point is also proved in the reference (Jung et al., 2015). As the live load is amplified by 10 times, the cable tension difference reduces from 3.9% to 0.8%, which is negligible.

In this paper, therefore, a modified deflection theory is to be proposed. It aims at the following three targets: considering the initial camber appropriately; considering the hanger extension realistically; and developing an easy-to-apply procedure for the preliminary design, without solving the complex nonlinear equations, by neglecting the tower flexural stiffness. The verification of the modified deflection theory will be examined carefully.

The remainder of this paper is organized as follows. First, in Section 1, the bridge model for analysis is developed and the employed assumptions are summarised. Then in Section 2, the modified deflection theory is formulated. Its solution procedure is presented in Section 3. In Section 4, comparisons of the solutions between the modified deflection theory and the previous one are made by an example design. Finally, some conclusions are drawn.

1. Bridge model and assumptions

Figure 1 shows the idealized plane model for the self-anchored suspension bridge. It is a typical three-span suspension bridge consisting of two towers, one continuous main girder, one main cable, and a series of hangers. The main cable is anchored at both ends of the main girder and the main girder is supported at the two towers and the two ends. The supports are rollers except for a hinged support at the left tower. The black solid lines denote the initial configuration of the bridge under dead loads considering the initial fabrication camber w_0, and the red dashed lines denote the deformed configuration of the bridge after the application of live loads.

In order to derive the modified deflection theory, the following reasonable assumptions are made:

1. The dead loads of the main girder, main cable and hangers are all uniformly distributed, and the main girder is at a zero-flexural stress state under the dead loads. Consequently, all the dead loads are carried by the main cable eventually;
2. The hangers are vertical under the dead loads and remain vertical under the live loads;
3. The materials of the bridge remain linear elastic under the live loads;

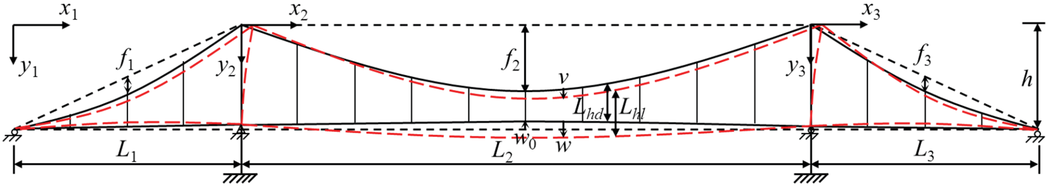

Figure 1. A typical three-span self-anchored suspension bridge model

4. The cross section and elastic modulus of the main girder are constant along the bridge spans;
5. The tower flexural stiffness is neglected, as discussed earlier.

2. Modified deflection theory

The entire bridge system can be decomposed into two subsystems: the main cable and the main girder. Their sectional free body diagrams, as well as those of the hanger, under both the dead loads and the dead and live loads are shown in Figure 2, where w_g, w_c and w_h denote the uniformly distributed self-weights of the main girder, main cable and hangers, respectively, and $q_d = w_g + w_c + w_h$ is the total dead load per unit length. According to Assumption (1), the main girder is at a zero-flexural stress state under the dead loads, so the tension at the bottom of the hanger is $T_{hb} = w_g$, and in turn the tension at the top of the hanger is $T_{ht} = w_g + w_h$. After the live load $q_l(x)$ is applied to the main girder, the hanger tension is increased by $q_h(x)$. Now the fundamental equations of the main cable and the main girder are formulated as follows.

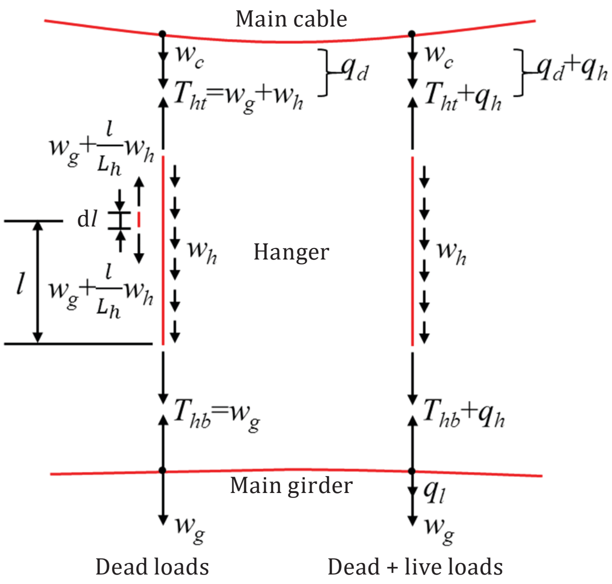

Figure 2. Free body diagrams of main cable, main girder and hanger

2.1. Main cable

With Assumption (1) and the parabolic cable theory (Irvine, 1981), the equilibrium equation of the main cable under the dead loads is given by

$$-H_d y'' = q_d, \tag{1}$$

where H_d is the horizontal component of the cable tension under the dead loads and y is the cable profile under the dead loads with positive direction downwards. The superscript $'$ denotes differentiation with respect to the horizontal ordinate x_i (i = 1, 2, 3), as shown in Figure 1.

Considering the cable geometry:

$$y_1 = -\frac{4f_1}{L_1^2}x_1^2 + \frac{4f_1 - h}{L_1}x_1 + h, \tag{2}$$

$$y_2 = -\frac{4f_2}{L_2^2}x_2^2 + \frac{4f_2}{L_2}x_2, \tag{3}$$

$$y_3 = -\frac{4f_3}{L_3^2}x_3^2 + \frac{4f_3 + h}{L_3}x_3, \tag{4}$$

where h is the tower height above the main girder, L_1, L_2 and L_3 are the span lengths of each span, respectively, and f_1, f_2 and f_3 are the sag lengths of each span, respectively, the horizontal cable force under the dead loads is

$$H_d = \frac{q_d L_1^2}{8f_1} = \frac{q_d L_2^2}{8f_2} = \frac{q_d L_3^2}{8f_3}. \tag{5}$$

After the live load is applied to the main girder, the hanger tension is increased by $q_h(x)$. Thus, the equilibrium equation of the main cable is

$$-(H_d + H_l)(y'' + v'') = q_d + q_h(x), \tag{6}$$

where H_l is the additional horizontal cable force due to the live load and v is the vertical deflection of the cable under the live load with positive direction downwards, as shown in Figure 1.

2.2. Main girder

According to Assumption (1), the main girder is at a zero-flexural stress state under the dead loads. Based on the classical beam-column theory (Timoshenko, 1947), its equilibrium equation considering the initial fabrication camber $w_0(x)$ is given by

$$E_g I_g w_0'''' + H_d w_0'' = T_{hb} - w_g = 0, \tag{7}$$

where E_g and I_g are the elastic modulus and area moment of inertia of the main girder, respectively, and w_0 is positive in the upward direction.

The term $H_d w_0''$ stems from the contribution of the compression in the main girder, and it is the major difference between the self- and earth-anchored suspension bridges.

Then the live load $q_l(x)$ is applied, and the equilibrium equation of the main girder is similarly given by

$$E_g I_g (w - w_0)'''' + (H_d + H_l)(w - w_0)'' = q_l(x) + w_g - T_{hb} - q_h(x), \tag{8}$$

where w is the vertical deflection of the main girder under the live load with positive direction downwards, as shown in Figure 1.

Eliminating $w_g - T_{hb}$ from Equations (7) and (8) leads to

$$E_g I_g w'''' + (H_d + H_l) w'' = q_l(x) - q_h(x) + H_l w_0''. \tag{9}$$

The last term in the equation reflects the effects of the initial camber.

2.3. Deformation compatibility

There are two deformation compatibility conditions under the live load. First, the vertical deflection of the main girder, w, is equal to that of the main cable, v, plus the hanger extension $L_{hl} - L_{hd}$ where $L_{hd} = h - y - w_0$ is the hanger length under the dead loads and L_{hl} is the hanger length after the extension due to the live load, as illustrated in Figure 1. Second, the horizontal projection of the change in cable length is equal to the shortening of the main girder. They are examined respectively in the following subsections.

2.3.1. First deformation compatibility condition

The free length of the hanger without any tension is assumed to be $L_h(x)$. Under the dead loads, the free body diagram of an infinitesimal length of the hanger with a distance l to the hanger bottom is also shown in Figure 2. The extension of the infinitesimal length is given by

$$\frac{w_g + w_h l / L_h}{E_h A_h} \mathrm{d}l,$$

where E_h and A_h are the elastic modulus and cross-sectional area of the hanger, respectively. Then the total length of the hanger is

$$L_{hd} = h - y - w_0 = L_h + \int_0^{L_h} \frac{w_g + w_h l / L_h}{E_h A_h} \mathrm{d}l = L_h \left(1 + \frac{w_g + w_h / 2}{E_h A_h}\right). \tag{10}$$

Similarly, after the live load is applied, the total length of the hanger is

$$L_{hl} = L_h \left(1 + \frac{w_g + q_h + w_h / 2}{E_h A_h}\right). \tag{11}$$

Therefore, the first deformation compatibility condition can be expressed as

$$v = w - \left(L_{\mathrm{hl}} - L_{\mathrm{hd}}\right) = w - \frac{q_{\mathrm{h}}(x)(h - y - w_0)}{E_{\mathrm{h}} A_{\mathrm{h}} + w_{\mathrm{g}} + w_{\mathrm{h}} / 2}. \tag{12}$$

2.3.2. Second deformation compatibility condition

The horizontal projection of the elongation in an infinitesimal cable length under the live load is given by (Irvine, 1981)

$$\mathrm{d}u = \frac{H_{\mathrm{l}}\left(1 + y'^2\right)^{\frac{3}{2}}}{E_{\mathrm{c}} A_{\mathrm{c}}} \mathrm{d}x - y' \mathrm{d}v - \frac{1}{2} v'^2 \mathrm{d}x, \tag{13}$$

where E_{c} and A_{c} are the elastic modulus and cross-sectional area of the main cable, respectively.

Integrating the above equation over each span length and using the integration by parts and Equation (1), the second deformation compatibility condition is written as

$$\sum_{i=1}^{3}\left(-\frac{H_{\mathrm{l}}}{E_{\mathrm{c}} A_{\mathrm{c}}} \int_0^{L_i} \left(1 + y_i'^2\right)^{\frac{3}{2}} \mathrm{d}x_i + \frac{q_{\mathrm{d}}}{H_{\mathrm{d}}} \int_0^{L_i} v_i \, \mathrm{d}x_i + \frac{1}{2} \int_0^{L_i} v_i'^2 \, \mathrm{d}x_i\right) =$$

$$= \sum_{i=1}^{3}\left(\frac{H_{\mathrm{l}} L_i}{E_{\mathrm{g}} A_{\mathrm{g}}} + \frac{1}{2} \int_0^{L_i} \left(w_i - w_{0i}\right)'^2 \mathrm{d}x_i\right), \tag{14}$$

where A_{g} is the cross-sectional area of the main girder. The second term on the right-hand side of the equation accounts for the additional shortening of the main girder due to its deflection. Note that when the total horizontal change of the cable length in the three spans, instead of the change in each span, is expressed, the contribution of the horizontal displacements at the tower tops is readily cancelled out.

3. Solution of the modified deflection theory

Combining Equations (6), (9), (12) and (14), there are four unknowns, i.e., H_{l}, $q_{\mathrm{h}}(x)$, v, and w, in the four equations. They should be solvable, as illustrated subsequently, with appropriate boundary conditions.

First, adding Equations (6) and (9) and using Equation (1) by eliminating $q_\mathrm{h}(x)$ and y'' yield

$$E_\mathrm{g}I_\mathrm{g}w'''' + \left(H_\mathrm{d}+H_\mathrm{l}\right)\left(w-v\right)'' = q_\mathrm{l}\left(x\right) - \frac{H_\mathrm{l}}{H_\mathrm{d}}q_\mathrm{d} + H_\mathrm{l}w_0''. \tag{15}$$

Note that if the hanger extension is neglected, i.e., $w = v$, Equation (15) is reduced to

$$E_\mathrm{g}I_\mathrm{g}w'''' = q_\mathrm{l}\left(x\right) - \frac{H_\mathrm{l}}{H_\mathrm{d}}q_\mathrm{d} + H_\mathrm{l}w_0'', \tag{16}$$

which has a similar form to Equation (9b) in the reference (Jung et al., 2015) except that now the horizontal cable tension under the dead loads, H_d, is irrelevant to the initial camber and the equation is related to the whole camber function by the additional last term. Since in practice the live loads are generally uniform and the initial camber is at most parabolic, the right-hand side of Equation (16) is constant and its solution is given by

$$w = \frac{A}{6}x^3 + \frac{B}{2}x^2 + Cx + D + \frac{H_\mathrm{d}q_\mathrm{l} - H_\mathrm{l}q_\mathrm{d} + H_\mathrm{d}H_\mathrm{l}w_0''}{24E_\mathrm{g}I_\mathrm{g}H_\mathrm{d}}x^4, \tag{17}$$

where A, B, C and D are constants determined by the boundary conditions. It is known from Equation (17) that the deflection of the main cable and girder is a fourth-order polynomial when the hanger extension is not considered. Afterwards, the hanger tension increment $q_\mathrm{h}(x)$ in this case can be extracted from Equation (6) or (9) and the bending moment of the main girder is obtained by integrating Equation (16) twice, i.e. $M(x) = -E_\mathrm{g}I_\mathrm{g}w''$.

On the other hand, if the hanger extension is considered, then from Equation (12),

$$v'' = w'' - \frac{q_\mathrm{h}''\left(h-y-w_0\right) - 2q_\mathrm{h}'\left(y'+w_0'\right) - q_\mathrm{h}\left(y''+w_0''\right)}{E_\mathrm{h}A_\mathrm{h} + w_\mathrm{g} + w_\mathrm{h}/2}. \tag{18}$$

Substituting Equation (18) into Equation (15) yields

$$\begin{aligned} E_\mathrm{g}I_\mathrm{g}w'''' &= q_\mathrm{l}\left(x\right) - \frac{H_\mathrm{l}}{H_\mathrm{d}}q_\mathrm{d} - \\ &-\left(H_\mathrm{d}+H_\mathrm{l}\right)\frac{q_\mathrm{h}''\left(h-y-w_0\right) - 2q_\mathrm{h}'\left(y'+w_0'\right) - q_\mathrm{h}\left(y''+w_0''\right)}{E_\mathrm{h}A_\mathrm{h} + w_\mathrm{g} + w_\mathrm{h}/2} + H_\mathrm{l}w_0''. \end{aligned} \tag{19}$$

Using Equation (9) again by eliminating $q_\mathrm{h}(x)$, a sixth-order variable-coefficient ordinary differential equation of w with respect to x is obtained as follows:

$$\frac{E_g I_g (H_d + H_l)}{E_h A_h + w_g + w_h / 2}(h - y - w_0) w^{VI} - \frac{2E_g I_g (H_d + H_l)}{E_h A_h + w_g + w_h / 2}(y' + w_0') w^{V} +$$
$$+\left[\frac{(H_d + H_l)^2}{E_h A_h + w_g + w_h / 2}(h - y - w_0) - \frac{E_g I_g (H_d + H_l)}{E_h A_h + w_g + w_h / 2}(y'' + w_0'') - E_g I_g\right] w'''' -$$
$$-\frac{2(H_d + H_l)^2}{E_h A_h + w_g + w_h / 2}(y' + w_0') w''' - \frac{(H_d + H_l)^2}{E_h A_h + w_g + w_h / 2}(y'' + w_0'') w'' =$$
$$= -q_l(x) + \frac{H_l}{H_d} q_d - H_l w_0'' +$$
$$+(H_d + H_l)\frac{(q_l'' + H_l w_0'''')(h - y - w_0) - 2(q_l' + H_l w_0''')(y' + w_0') - (q_l + H_l w_0'')(y'' + w_0'')}{E_h A_h + w_g + w_h / 2}, \quad (20)$$

where the superscripts “VI” and “V” denote the sixth- and fifth-order differentiation, respectively.

The equation above is a complicated variable-coefficient differential equation whose exact analytical solution is difficult to attain. It can be solved numerically, but that is still demanding for the preliminary design. Fortunately, inspired by Equation (17) that the deflection of the main girder should be close to a fourth-order polynomial even the hanger extension is considered, we are able to seek an approximate solution here by omitting the sixth- and fifth-order differentiation terms in Equation (20). Also, by knowing that in practice the live loads are generally uniform and the initial camber is at most parabolic and by introducing $z = w''$, Equation (20) is reduced to a second-order variable-coefficient differential equation as follows:

$$\left[\frac{(H_d + H_l)^2}{E_h A_h + w_g + w_h / 2}(h - y - w_0) - \frac{E_g I_g (H_d + H_l)}{E_h A_h + w_g + w_h / 2}(y'' + w_0'') - E_g I_g\right] z'' -$$
$$-\frac{2(H_d + H_l)^2}{E_h A_h + w_g + w_h / 2}(y' + w_0') z' - \frac{(H_d + H_l)^2}{E_h A_h + w_g + w_h / 2}(y'' + w_0'') z =$$
$$= -q_l + \frac{H_l}{H_d} q_d - H_l w_0'' - \frac{(H_d + H_l)(q_l + H_l w_0'')(y'' + w_0'')}{E_h A_h + w_g + w_h / 2}. \quad (21)$$

The analytical solution to Equation (21) is available. Assuming that the cable geometry and initial camber are expressed as the following forms:

$$y = a_1 x^2 + a_2 x + a_3, \quad (22)$$

$$w_0 = b_1 x^2 + b_2 x + b_3, \quad (23)$$

the solution to Equation (21) is written as

$$z=\frac{Am_1x+Bm_1+m_2x^2}{n_1x^2+n_2x+n_3}, \tag{24}$$

where

$$m_1=2\left(E_\mathrm{h}A_\mathrm{h}+w_\mathrm{g}+w_\mathrm{h}/2\right)H_\mathrm{d}, \tag{25}$$

$$m_2=\left(E_\mathrm{h}A_\mathrm{h}+w_\mathrm{g}+w_\mathrm{h}/2\right)\left(H_\mathrm{d}q_\mathrm{l}-H_\mathrm{l}q_\mathrm{d}\right)+2\left(H_\mathrm{d}^2+H_\mathrm{d}H_\mathrm{l}\right)q_\mathrm{l}\left(a_1+b_1\right)+$$
$$+4H_\mathrm{d}H_\mathrm{l}\left(H_\mathrm{d}+H_\mathrm{l}\right)\left(a_1b_1+b_1^2\right)+2\left(E_\mathrm{h}A_\mathrm{h}+w_\mathrm{g}+w_\mathrm{h}/2\right)H_\mathrm{d}H_\mathrm{l}b_1, \tag{26}$$

$$n_1=2H_\mathrm{d}\left(H_\mathrm{d}+H_\mathrm{l}\right)^2\left(a_1+b_1\right), \tag{27}$$

$$n_2=2H_\mathrm{d}\left(H_\mathrm{d}+H_\mathrm{l}\right)^2\left(a_2+b_2\right), \tag{28}$$

$$n_3=2H_\mathrm{d}\left(a_3+b_3-h\right)\left(H_\mathrm{d}^2+H_\mathrm{l}^2\right)+4H_\mathrm{d}E_\mathrm{g}I_\mathrm{g}\left(a_1+b_1\right)\left(H_\mathrm{d}+H_\mathrm{l}\right)+$$
$$+4H_\mathrm{d}^2H_\mathrm{l}\left(a_3+b_3-h\right)+2H_\mathrm{d}E_\mathrm{g}I_\mathrm{g}\left(E_\mathrm{h}A_\mathrm{h}+w_\mathrm{g}+w_\mathrm{h}/2\right). \tag{29}$$

Integrating Equation (22) twice, the deflection of the main girder is obtained by

$$w=\frac{m_2x^2}{2n_1}+k_1\left(x-\Delta_1\right)\ln\left(x-\Delta_1\right)-k_1x+$$
$$+k_2\left(x-\Delta_2\right)\ln\left(\Delta_2-x\right)-k_2x+Cx+D, \tag{30}$$

where

$$\Delta_1=\frac{-n_2+\sqrt{n_2^2-4n_1n_3}}{2n_1}, \tag{31}$$

$$\Delta_2=\frac{-n_2-\sqrt{n_2^2-4n_1n_3}}{2n_1}, \tag{32}$$

$$k_1=\frac{Am_1n_1\sqrt{n_2^2-4n_1n_3}-Am_1n_1n_2+2Bm_1n_1^2-2m_2n_1n_3+m_2n_2^2-m_2n_2\sqrt{n_2^2-4n_1n_3}}{2n_1^2\sqrt{n_2^2-4n_1n_3}}, \tag{33}$$

$$k_2=\frac{Am_1n_1\sqrt{n_2^2-4n_1n_3}+Am_1n_1n_2-2Bm_1n_1^2+2m_2n_1n_3-m_2n_2^2-m_2n_2\sqrt{n_2^2-4n_1n_3}}{2n_1^2\sqrt{n_2^2-4n_1n_3}}. \tag{34}$$

Equation (30) is the practical approximate solution sought for the main girder deflection. The constants A, B, C and D can be determined by the boundary conditions of the continuous main girder. For instance, for a fully uniform live load in each span, the twelve constants A_i, B_i, C_i and D_i ($i=1, 2, 3$) are determined by the following twelve boundary conditions:

$$w_1\left(0\right)=0,\ w_1\left(L_1\right)=0,\ w_2\left(0\right)=0,\ w_2\left(L_2\right)=0,$$
$$w_3\left(0\right)=0,\ w_3\left(L_3\right)=0,\ w_1'\left(L_1\right)=w_2'\left(0\right),\ w_2'\left(L_2\right)=w_3'\left(0\right),$$
$$w_1''\left(0\right)=0,\ w_3''\left(L_3\right)=0,\ w_1''\left(L_1\right)=w_2''\left(0\right),\ w_2''\left(L_2\right)=w_3''\left(0\right). \tag{35}$$

Subsequently, substituting Equation (30) into Equation (9) yields the hanger tension increment $q_h(x)$ as follows:

$$q_h = E_g I_g \left[\frac{2k_1}{(\Delta_1 - x)^3} + \frac{2k_2}{(\Delta_2 - x)^3} \right] + \\ + (H_d + H_l)\left(\frac{k_1}{\Delta_1 - x} + \frac{k_2}{\Delta_2 - x} - \frac{m_2}{n_1} \right) + q_l + 2H_l b_1. \quad (36)$$

Therefore, the deflection of the main cable v is obtained by Equation (12). The second term on the right-hand side of Equation (12) reflects the deflection difference between the main cable and the main girder, i.e., the hanger extension.

The girder deflection w_i, Equation (30), and the cable deflection v_i are both expressed in terms of H_l. Substituting them into the second deformation compatibility Equation (14), there is only one unknown H_l. Consequently, the additional girder compression due to the live load is obtained. Plugging H_l back into w_i, v_i and Equation (36), the girder deflection, cable deflection and hanger tension increment q_h for each span are all gained. Finally, integrating Equation (15) twice results in the bending moment of the main girder as follows:

$$M(x) = -E_g I_g w'' - (H_d + H_l)(w - v). \quad (37)$$

The entire solution procedure above can be easily coded as a simple computer program and its flow is summarised as follows:

- *Step 1*: Start. Input geometric, loading and material properties.
- *Step 2*: Solve Equation (30) for the constants A, B, C and D of w_i using the continuous boundary conditions of the main girder, e.g., Equation (35). The solved w_i is expressed in terms of H_l.
- *Step 3*: Solve Equation (12) for v_i using the solved Equations (30) and (36). The solved v_i is also expressed in terms of H_l.
- *Step 4*: Solve Equation (14) for H_l and thus w_i, v_i and q_h are known.
- *Step 5*: Solve Equation (37) for M.
- *Step 6*: Output results. End.

4. Verification example

To verify the modified deflection theory, the same bridge example investigated by Jung et al. (2015) is chosen here for comparison. Its geometric, loading, and material properties are listed in Table 1.

Figure 3 plots the deflections of the main cable and girder computed by the modified deflection theory considering and not considering the hanger extension, i.e., Equation (15) vs. Equation (16). For this example, the hanger extension is not significant, but obviously when the hanger extension is considered, the bridge system is more flexible and, thus, the maximum downward deflection is increased from 3.623 m to 3.662 m. In addition, by plugging the computed deflections back into the original sixth-order variable-coefficient differential Equation (20), it is found that the value of the sixth- and fifth-order differentiation terms is far smaller than that of the rest terms. Therefore, the approximation made earlier to solve the equation is rational.

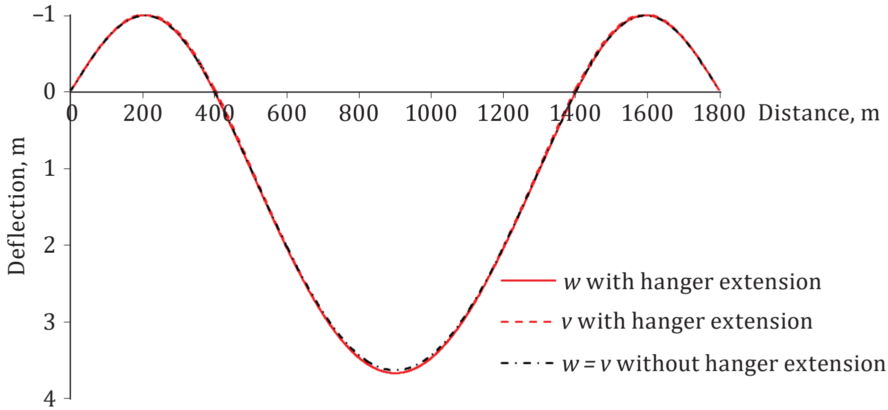

Figure 3. Deflections of the main cable and girder

Table 1. Geometric, loading and material properties of a bridge example

Property	Value	Property	Value
Centre span length L_2, m	1000	Initial camber w_{03}, m	$-0.02x_3+8$
Side span lengths L_1 and L_3, m	400	Centre live load q_{l2}, kN/m	127
Centre sag length f_2, m	170	Side live loads q_{l1} and q_{l3}, kN/m	0
Side sag lengths f_1 and f_3, m	27.2	Cable modulus E_c, GPa	196.20
Tower height h, m	185	Cable area A_c, m^2	0.516
Cable weight w_c, kN/m	59.48	Girder modulus E_g, GPa	206.01
Girder weight w_g, kN/m	445.18	Girder area A_g, m^2	1.363
Hanger weight w_h, kN/m	5.88	Girder moment I_g, m^4	217.39
Total dead load q_d, kN/m	510.54	Hanger modulus E_h, GPa	137.34
Initial camber w_{01}, m	$0.02x_1$	Hanger area A_h, m^2	0.051
Initial camber w_{02}, m	$-0.00002(x_2-500)^2+13$	Hanger spacing, m	20

Table 2. Comparison of solutions using different theories

Solution	Present with hanger extension	Present without hanger extension	Previous (Jung et al., 2015)	FEM (Jung et al., 2015)
H_l, MN	74.099 (–0.4%)	74.494 (0.2%)	79.671 (7.1%)	74.369
w_{2max}, m	3.662 (8.9%)	3.623 (7.8%)	3.259 (–3.1%)	3.362
$w_{1max} = w_{3max}$, m	–0.998 (8.0%)	–0.994 (7.6%)	–0.977 (5.7%)	–0.924
v_{2max}, m	3.661	3.623	3.259	Not given
$v_{1max} = v_{3max}$, m	–1.012	–0.994	–0.977	Not given
M_{2max}, MN-m	1792.2 (6.3%)	1771.1 (5.0%)	1556.0 (–7.7%)	1686.4
$M_{1max} = M_{3max}$, MN-m	–2611.9 (8.3%)	–2595.1 (7.6%)	–2563.2 (6.3%)	–2412.3

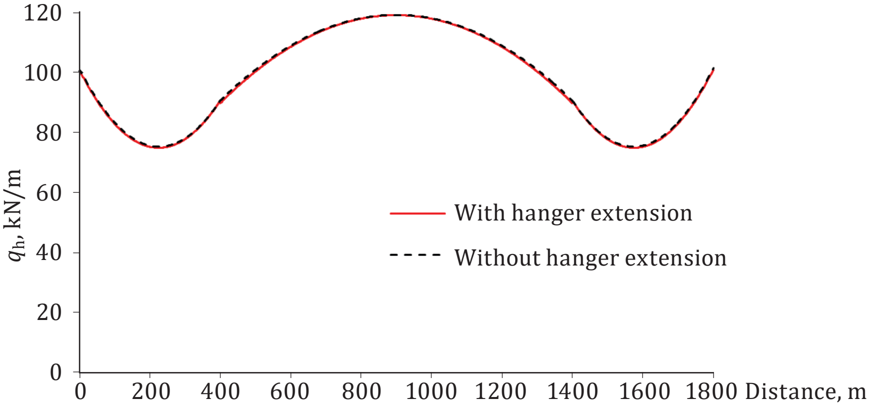

Figure 4. Hanger tension increment of the self-anchored suspension bridge

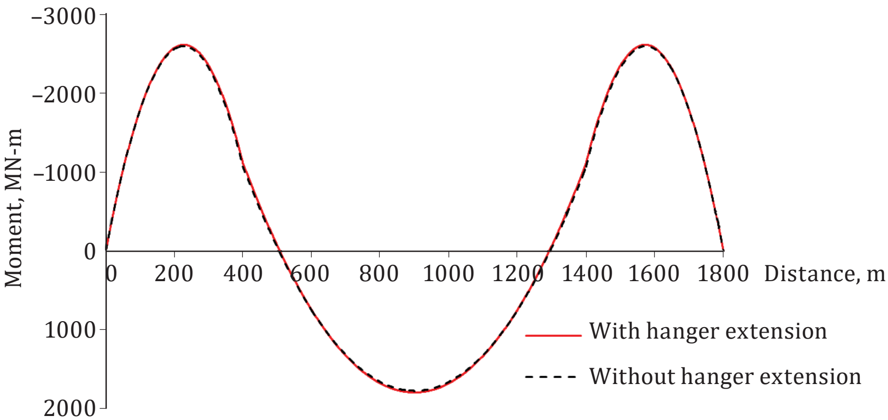

Figure 5. Bending moment of the main girder

Meanwhile, for this bridge example, the maximum hanger extension $w-v$ is 0.045 m, locating near the towers. From Equation (12), the specific value of the hanger extension is dependent on the hanger tension increment q_h, so Figure 4 plots the distributions of the hanger tension increment considering and not considering the hanger extension. The former is smaller than the latter.

Figure 5 shows the bending moment of the main girder. It can be seen that for the given live load, the maximum positive bending moment is increased from 1771.1 MN-m to 1792.2 MN-m and the maximum negative bending moment is increased from −2595.1 MN-m to −2611.9 MN-m when the hanger extension is considered.

Finally, for comparison, the present results computed by the modified deflection theory considering and not considering the hanger extension, as well as those from the previous deflection theory and complex finite element analysis (Jung et al., 2015), are listed in Table 2. The percentage in the brackets denotes the relative errors to the FEM solutions. It is observed that the present theory gives much closer additional horizontal cable force H_l to the FEM solution than the previous one. This indirectly confirms the appropriate consideration of the initial camber in the present theory. Moreover, the modified theory leads to larger deflection and bending moment of the main girder, which is more conservative for the preliminary design. Especially, if the deflection difference between the main cable and the main girder cannot be neglected in the design, the difference is properly considered in the proposed theory.

Conclusions

The study has proposed a modified deflection theory, considering the initial camber appropriately, taking the hanger extension into account and neglecting the tower flexural stiffness, for the preliminary design of self-anchored suspension bridge. It consists of force equilibrium and deformation compatibility of the whole bridge system. The theory leads to a complicated sixth-order variable-coefficient differential equation eventually. A practical approximate solution to the differential equation is obtained. To verify the solution, a bridge example is examined. Through comparison of results between the modified deflection theory and the previous one, some conclusions are drawn as follows:

1. The proposed deflection theory is effective and easy-to-use. It well predicts the additional horizontal cable force, the deflections of the main cable and girder and the bending moment of the main girder, and it does not require to solve nonlinear equations;

2. The modified deflection theory gives closer additional horizontal cable force to the FEM solution than the previous theory;
3. The modified deflection theory gives more conservative deflections and bending moment due to the consideration of the hanger extension;
4. When the deflection difference between the main cable and the main girder is considerable, the modified deflection theory is capable of predicting the difference.

REFERENCES

Buonopane, S. G., and Billington, D. P. (1993). Theory and history of suspension bridge design from 1823 to 1940. *Journal of Structural Engineering*, *119*(3), 954–977. https://doi.org/10.1061/(ASCE)0733-9445(1993)119:3(954)

Chen, Y., Wang, S., Zhong, J., and Lian, F. (2022). Study on static analytical method of multi-tower self-anchored suspension bridge. *Applied Sciences*, *12*(17), Article 8499. https://doi.org/10.3390/app12178499

Choi, D. H., Gwon, S. G., Yoo, H., and Na, H. S. (2013). Nonlinear static analysis of continuous multi-span suspension bridges. *International Journal of Steel Structures*, *13*(1), 103–115. https://doi.org/10.1007/s13296-013-1010-0

Clemente, P., Nicolosi, G., and Raithel, A. (2000). Preliminary design of very long-span suspension bridges. *Engineering Structures*, *22*(12), 1699–1706. https://doi.org/10.1016/S0141-0296(99)00112-1

Cobo del Arco, D., and Aparicio, A. C. (2001). Preliminary static analysis of suspension bridges. *Engineering Structures*, *23*(9), 1096–1103. https://doi.org/10.1016/S0141-0296(01)00009-8

Gwon, S. G., and Choi, D. H. (2018). Static and dynamic analyses of a suspension bridge with three-dimensionally curved main cables using a continuum model. *Engineering Structures*, *161*, 250–264. https://doi.org/10.1016/j.engstruct.2018.01.062

Han, Y., Chen, Z., Luo, S., and Yang, S. (2009). Calculation method on shape finding of self-anchored suspension bridge with spatial cables. *Frontiers of Architecture and Civil Engineering in China*, *3*(2), 165–172. https://doi.org/10.1007/s11709-009-0021-6

Irvine, H. M. (1981). *Cable structures*. Cambridge: The MIT Press.

Jennings, A. (1987). Deflection theory analysis of different cable profiles for suspension bridges. *Engineering Structures*, *9*(2), 84–94. https://doi.org/10.1016/0141-0296(87)90002-2

Jung, M. R., Jang, M. J., Attard, M. M., and Kim, M. Y. (2017). Elastic stability behavior of self-anchored suspension bridges by the deflection theory. *International Journal of Structural Stability and Dynamics*, *17*(4), Article 1750050. https://doi.org/10.1142/S021945541750050X

Jung, M. R., Shin, S. U., Attard, M. M., and Kim, M. Y. (2015). Deflection theory for self-anchored suspension bridges under live load. *Journal of Bridge Engineering*, *20*(7), Article 04014093. https://doi.org/10.1061/(ASCE)BE.1943-5592.0000687

Kim, M. Y., Jung, M. R., and Attard, M. M. (2019). Unstrained length-based methods determining an optimized initial shape of 3-dimensional self-anchored suspension bridges. *Computers and Structures*, *217*, 18–35. https://doi.org/10.1016/j.compstruc.2019.03.008

Kim, H. K., and Kim, M. Y. (2012). Efficient combination of a TCUD method and an initial force method for determining initial shapes of cable-supported bridges. *International Journal of Steel Structures*, *12*(2), 157–174. https://doi.org/10.1007/s13296-012-2002-1

Kim, H. K., Lee, M. J., and Chang, S. P. (2002). Non-linear shape-finding analysis of a self-anchored suspension bridge. *Engineering Structures*, *24*(12), 1547–1559. https://doi.org/10.1016/S0141-0296(02)00097-4

Kim, H. K., Lee, M. J., and Chang, S. P. (2006). Determination of hanger installation procedure for a self-anchored suspension bridge. *Engineering Structures*, *28*(7), 959–976. https://doi.org/10.1016/j.engstruct.2005.10.019

Li, T., and Liu, Z. (2021). An improved continuum model for determining the behavior of suspension bridges during construction. *Automation in Construction*, *127*, Article 103715. https://doi.org/10.1016/j.autcon.2021.103715

Ochsendorf, J. A., and Billington, D. P. (1999). Self-anchored suspension bridges. *Journal of Bridge Engineering*, *4*(3), 151–156. https://doi.org/10.1061/(ASCE)1084-0702(1999)4:3(151)

Romeijn, A., Sarkhosh, R., and Van Goolen, D. (2008). Parametric study on static behaviour of self-anchored suspension bridges. *International Journal of Steel Structures*, *8*(2), 91–108. http://www.kssc.or.kr/wonmun/KSSC_3_2008_8_2_91(C).pdf

Shin, S. U., Jung, M. R., Park, J., and Kim, M. Y. (2015). A deflection theory and its validation of earth-anchored suspension bridges under live loads. *KSCE Journal of Civil Engineering*, *19*(1), 200–212. https://doi.org/10.1007/s12205-014-0641-9

Sun, Y., Zhu, H. P., and Xu, D. (2015). New method for shape finding of self-anchored suspension bridges with three-dimensionally curved cables. *Journal of Bridge Engineering*, *20*(2), Article 04014063. https://doi.org/10.1061/(ASCE)BE.1943-5592.0000642

Timoshenko, S. (1947). *Strength of materials: Part II. Advanced theory and problems.* New York: D. Van Nostrand Company, Inc.

Ulstrup, C. C. (1993). Rating and preliminary analysis of suspension bridges. *Journal of Structural Engineering*, *119*(9), 2653–2679. https://doi.org/10.1061/(ASCE)0733-9445(1993)119:9(2653)

Wollmann, G. P. (2001). Preliminary analysis of suspension bridges. *Journal of Bridge Engineering*, *6*(4), 227–233. https://doi.org/10.1061/(ASCE)1084-0702(2001)6:4(227)

Zhang, W., Chang, J., and Feng, D. (2022). Determination of main cable shape and hanger tensions of a suspension bridge based on the measured live-load deflection of the main beam: An analytical algorithm. *Engineering Structures*, *272*, Article 115031. https://doi.org/10.1016/j.engstruct.2022.115031

Zhang, W., Chang, J., Lu, X., Tian, G., and Li, J. (2021). Suspension bridge deformation and internal forces under the concentrated live load: Analytical algorithm. *Engineering Structures*, *248*, Article 113271. https://doi.org/10.1016/j.engstruct.2021.113271

Zhuang, D., Xiao, R., Sun, B. and Yang, L. (2021). Concept and preliminary static analysis of hybrid anchored suspension bridge. *Journal of Bridge Engineering*, *26*(6), Article 04021032. https://doi.org/10.1061/(ASCE)BE.1943-5592.0001728